



## Stability of Red-Clay Slopes Subjected to Different Durations of Rainfall

Kaixi Xue, Binod Tiwari, Beena Ajmera, and Yanxiang Hu

### Abstract

The influence of long duration rainfall on the stability and deformation characteristics of red-clay slopes in China was evaluated using GeoStudio 2012. The 15 m tall modeled slope with a slope inclination of approximately  $37^\circ$  was subjected to rainfall at an intensity of  $6.25 \times 10^{-3}$  m/h for various durations. The durations examined in this study ranged between 1 day and 5 days. The pore water pressure and deformations resulting in the slope were evaluated using coupled and uncoupled analysis. Specifically, in the coupled analyses, the combined influence of seepage and deformation on the pore pressure, development of strains and the slope stability were examined. On the other hand, in the uncoupled analyses, only the influence of seepage on the pore pressure, strain development and factor of safety was considered. The results obtained suggest that the rate of pore pressure development was most significantly influenced when four days of rainfall was applied to the slope. The slope was found to settle following short duration rainfall events. However, the slope would swell during the long duration rainfall events. In these events, the greatest swelling was observed at the head of the slope. Similar to the pore pressure response, the factor of safety behaved hysterically with larger magnitudes noted in the coupled analysis in comparison to the uncoupled analysis.

### Keywords

Unsaturated soils • Rainfall infiltration • Slope stability • Red-clay slopes

K. Xue · Y. Hu

State Key Laboratory Breeding Base of Nuclear Resources and Environment, Civil and Architecture Engineering Department, East China University of Technology, 418 Guanglan Rd., Nanchang, 330013 Jiangxi, China  
e-mail: xkx1257@foxmail.com

Y. Hu

e-mail: hyx3461@foxmail.com

B. Tiwari

Department of Civil and Environmental Engineering, California State University, Fullerton, 800 N. State College Blvd., E-419, Fullerton, CA 92831, USA  
e-mail: btiwari@fullerton.edu

B. Ajmera (✉)

Department of Civil and Environmental Engineering, California State University, Fullerton, 800 N. State College Blvd., E-318, Fullerton, CA 92831, USA  
e-mail: bajmera@fullerton.edu

### Introduction

Rainfall-induced slope failures are one among the major geotechnical disasters causing significant loss of life, damage to infrastructure and economic losses. Among others, the 2014 Oso Landslide in Washington, USA (Haugerud 2014; Henn et al. 2015; Keaton et al. 2014; Wartman et al. 2016), the 1973 Attachie Landslide in British Columbia (Fletcher et al. 2002) and the 2005 La Conchita Landslide in California, USA are all documented cases of the major damage and destruction resulting from rainfall-induced slope failures. These slope failures typically occur during or after rainfall events that result in a loss of apparent cohesion in sediments from the infiltration of rainwater. In one of the first studies on rainfall-induced slope failures, erosion caused

by rainwater was found to be the cause of active sliding in areas with high rainfalls (Lumb 1962). In the fifty years since then, numerical simulations, laboratory scale models and centrifuge testing have provided insight into the influences of rainfall intensity, duration, antecedent rainfall and slope geometry on slope stability (Tiwari et al. 2013, 2014, 2016; Phommachanh et al. 2014; Hearn et al. 2014; Tran 2016).

The rainfall intensity, initial ground water table and the duration of the rainfall were found to control the stability of slopes (Ng and Shi 1998; Song et al. 2002; Wang and Liang 2010). In addition, the differences in the computed factors of safety resulting from numerical simulations considering hydro-mechanical coupling and uncoupling were greater as the intensity of rainfall increased (Liu et al. 2012). The effect of rainfall patterns on the stability of shallow slopes were studied using physical models by Brooks and Richards (1994) and Dhakal and Sidle (2004), who found variations in the depth and timing of instabilities with differences in the rainfall patterns. Similar conclusions were drawn by Tsai and Wang (2011), who showed differences in the depth and timing of instability with different rainfall patterns despite the same amount of rainfall application.

Although the duration and intensity of rainfall, rainfall patterns and slope geometry have been shown to affect the stability of slopes, extreme rainfall conditions have not been extensively examined in the previous work. Extreme rainfall conditions are defined as a series of long duration wetting and drying cycles. That is, rainfall will occur for a long duration followed by a long duration drying period. Previous studies have examined the variations in the pore water pressures as a result of wetting and drying cycles for transient seepage conditions, but an understanding of how coupling deformation and seepage will influence the stability of slopes is still lacking. In this study, pore water pressures and factors of safety for a red-clay slope in Jiangxi Province, China were examined using coupled deformation-seepage analyses and uncoupled seepage analyses.

(2014a), they were shown applicable for water flow through unsaturated soil by Brooks and Richards (1994). By solving the transient and two-dimension seepage analysis, the governing differential equation for water flow, as shown in Eq. (1), is derived. In Eq. (1),  $H$  is the total head,  $k_x$  and  $k_y$  are the hydraulic conductivities in the  $x$ - and  $y$ -directions, respectively,  $Q$  is the applied boundary flux,  $\gamma_w$  is the unit weight of water,  $m_w$  is the slope of the storage curve,  $y$  is the elevation and  $t$  is the time. In the derivation of Eq. (1), it is assumed that total stress conditions remain constant and that the pore-air pressure is equal to the atmospheric pressure during the entire transient process.

$$\frac{\partial}{\partial x} \left( k_x \frac{\partial H}{\partial y} \right) + \frac{\partial}{\partial y} \left( k_y \frac{\partial H}{\partial y} \right) + Q = m_w \gamma_w \frac{\partial H}{\partial t} \quad (1)$$

## Coupled Analyses Considering Seepage and Deformation

SIGMA/W of the GeoStudio suite (Geo-Slope International, Ltd. 2014b) was found to conduct the fully coupled analysis, which simultaneously considers the equations related to stress-deformation and seepage dissipation. The finite element equilibrium equations are determined using the principle of virtual work. Specifically, the total internal virtual work is set equal to the total external virtual work and results in Eq. (2) (Fredlund and Rahardjo 1993). In Eq. (2),  $[B]$  is the strain or gradient matrix,  $[D]$  is the drained constitutive matrix,  $[K]$  is the stiffness matrix,  $[L_d]$  is the coupling matrix,  $\{\Delta\delta\}$  is the incremental displacement vector and  $\{\Delta u_w\}$  is the incremental pore water pressure vector.

$$\begin{aligned} \sum [B]^T [D] [B] \{\Delta\delta\} + \sum [B]^T [D] \{m_h\} \langle N \rangle \{\Delta u_w\} &= \sum F \\ [K] &= [B]^T [D] [B] \\ [L_d] &= [B]^T [D] \{m_h\} \langle N \rangle \\ \{m_h\}^T &= \left\langle \frac{1}{H} \quad \frac{1}{H} \quad \frac{1}{H} \quad 0 \right\rangle \end{aligned} \quad (2)$$

## Background on Analyses Methods

### Uncoupled Analysis Considering Seepage Only

The fundamental flow laws for steady state and transient flow were used to conduct uncoupled analysis that consider seepage only using SEEP/W from the GeoStudio suite. Although these laws were originally derived from Darcy's laws for saturated conditions (Geo-Slope International, Ltd.

### Slope Stability

In this study, the general limit equilibrium methods available in SLOPE/W of the GeoStudio suite (Geo-Slope International, Ltd. 2014c) were used to determine the stability of the slope. Bishop's Method for stability analysis was adapted for this study. A modified version of the Mohr-Coulomb

equation, as presented in Eq. (3), was used to represent the shear strength of the unsaturated soil. In Eq. (3),  $S_m$  is the shear force mobilized on the base of each slice,  $\beta$  is the base length of each slice,  $F$  is the factor of safety,  $c'$  is the effective cohesion,  $\sigma_n$  is the total normal stress,  $u_a$  is the pore air pressure,  $\phi'$  is the effective angle of internal friction,  $u_w$  is the pore water pressure, and  $\phi^b$  is the angle defining the increase in the shear strength for an increase in the suction. When the pore water pressure was negative,  $\phi^b$  is used. On the other hand, when the pore water pressure was positive,  $\phi'$  is used.

$$S_m = \frac{\beta}{F} (c' + (\sigma_n - u_a) \tan \phi' + (u_a - u_w) \tan \phi^b) \quad (3)$$

## Methods

Based on the results of numerical simulations, Zhang et al. (2003) suggested that considerations to the slope geometry that would result in the best results from numerical simulations. In particular, it was recommended that the toe of the slope be at least 1.5 times the height of the slope away from the left boundary, while the head of the slope be located at least 2.5 times the height of the slope from the right boundary and at least 2 times the height of the slope away from the bottom boundary. The slope geometry used in this study is presented in Fig. 1 and adapts all of the suggestions provided by Zhang et al. (2003). The typical ground water conditions found in Jiangxi Province, China were used to determine the initial ground water table, also shown in Fig. 1. Locations T1–T7 represent the seven points at which the pore water pressure, water head, stress, strain and displacement was evaluated in this study.

The properties of the red-clay samples obtained from Jiangxi Province, China are summarized in Table 1. These properties were adapted in the numerical simulations. The soil is determined to classify as the silty sand (SM) material. Figure 2 contains the volumetric water content function, while Fig. 3 contains the hydraulic conductivity function. The hydraulic conductivity function was determined using the methods outlined by Fredlund and Xing (1994).

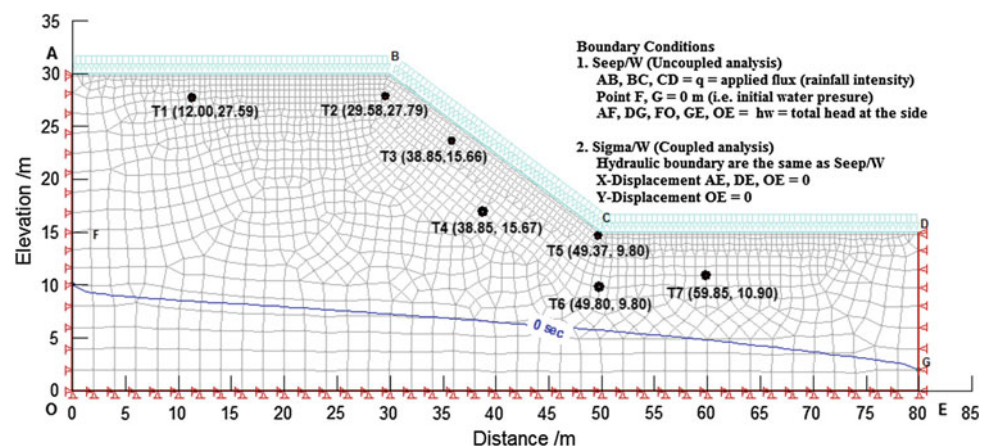
A rainfall intensity of 168.69 mm per day was found to be the extreme rainfall intensity in Chongqing City, China. The average rainstorm duration ranges between two to five days in Jiangxi Province. For this study, five rainfall durations of 1, 2, 3, 4 and 5 days with a rainfall intensity of  $6.25 \times 10^{-3}$  m/h was used in this study. Any rainfall lasting longer than three days is very unlikely, but such events are referred to as very long duration rainfall events.

## Results

### Pore Pressure Response

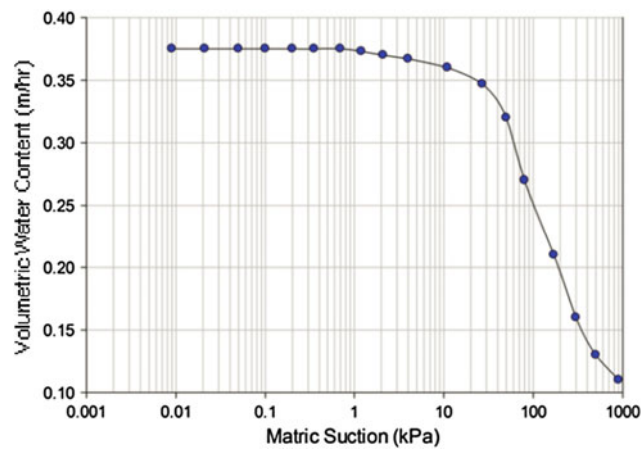
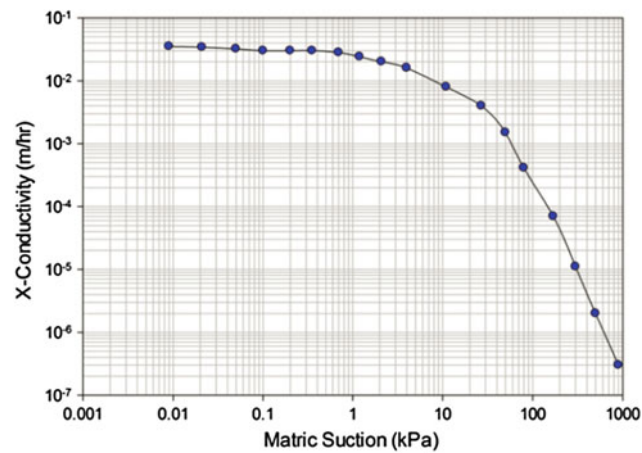
The locations of the water table during the five day rainstorms are shown in Fig. 4. As the rainstorm progressed, the water level was found to rise with the highest water level occurring on the fifth day. As the calculation period was extended, the water table would drop slightly. However, it continued to remain significantly higher than the initial ground water table. In the results from the coupled analysis shown in Fig. 4a, the water table was higher than that found from the uncoupled analysis (Fig. 4b). Differences between the coupled and uncoupled analyses were found to be insignificantly after steady-state conditions were achieved in approximately 10 days. Figure 5 contains the pore water

Fig. 1 Slope geometry



**Table 1** Properties of red-clay samples

Property	Value
Sand (%)	77
Fines (%)	23
Soil classification	SM
Saturated volumetric moisture content ( $\theta_w$ )	0.37
Saturated coefficient of permeability ( $k_s$ in m/h)	0.0323
Residual moisture content ( $\theta_r$ )	0.016
Unit weight ( $kN/m^3$ )	20
Friction angle ( $\varphi'$ in deg)	15
Cohesion ( $c'$ in kPa)	30
Effective modulus of elasticity ( $E'$ in MPa)	8.3
Poisson's ratio ( $\lambda$ )	0.334

**Fig. 2** Volumetric water content function**Fig. 3** Hydraulic conductivity function

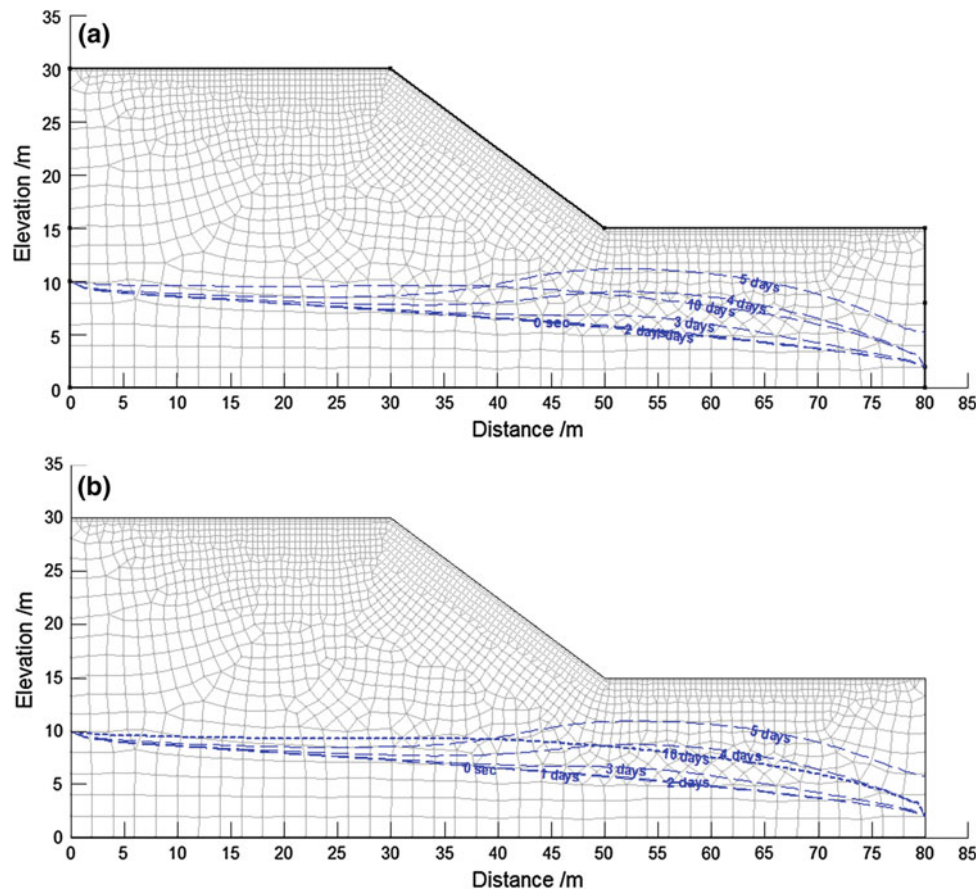


**Fig. 4** Rise in water table as observed through **a** coupled seepage-deformation and **b** uncoupled seepage only analyses

pressure response at the seven monitoring points identified in Fig. 1. It was found that the difference is the pore pressures at each point would decrease as the duration of the rainfall increased with the greatest changes occurring at T1, T2, and T3. It was found that the rainwater would continue to infiltrate after the end of the rainstorm.

### Distribution of Shear Strain

The infiltration of rainwater caused a variation in the unit weight of the red clay and a reduction in its shear strength with time resulting in shear strains along the slope. The magnitude of the horizontal (X), vertical (Y) and shear strain (XY) in the slope is presented in Figs. 6, 7, and 8, respectively. An increase in the duration of the rainfall resulted in an increase in the horizontal shear strains. Tensile strains up to 4% and compressive strains up to 2% were observed in

the slope. The toe of the slope was found to have the greatest vertical strain. The failure of the slope was found to initiate at the crest of the slope based on examinations of the shear strain development in the slope.

### Factor of Safety

An increase in the rainfall duration is shown to result in a decrease in the factor of safety, as shown in Fig. 9, which contains the relationship between the factor of safety and the duration of the rainfall. Table 2 summarizes the percentage reduction in the factor of safety with rainfall duration for the coupled and uncoupled analyses. It is seen that the coupled analysis shows a lower cumulative reduction in the factor of safety which is attributed to the changes in the void ratio resulting from infiltrating rainwater.



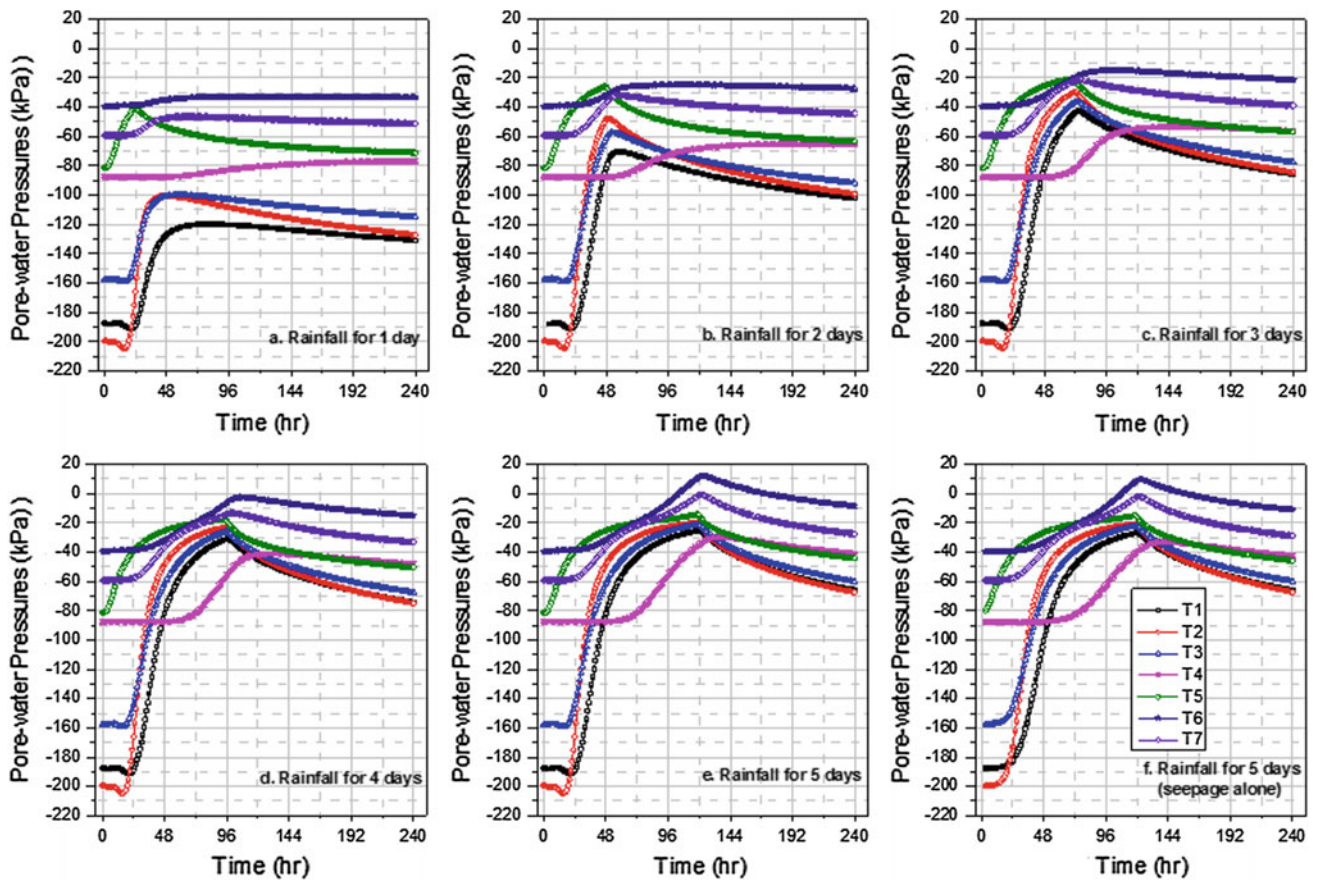


Fig. 5 Pore pressure at monitoring points for different rainstorm durations

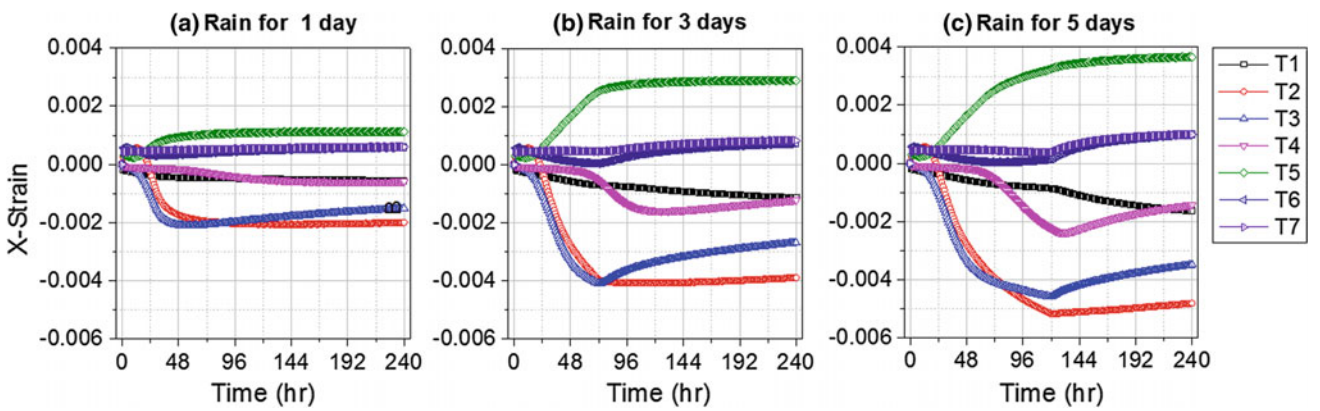


Fig. 6 Magnitude of horizontal strains

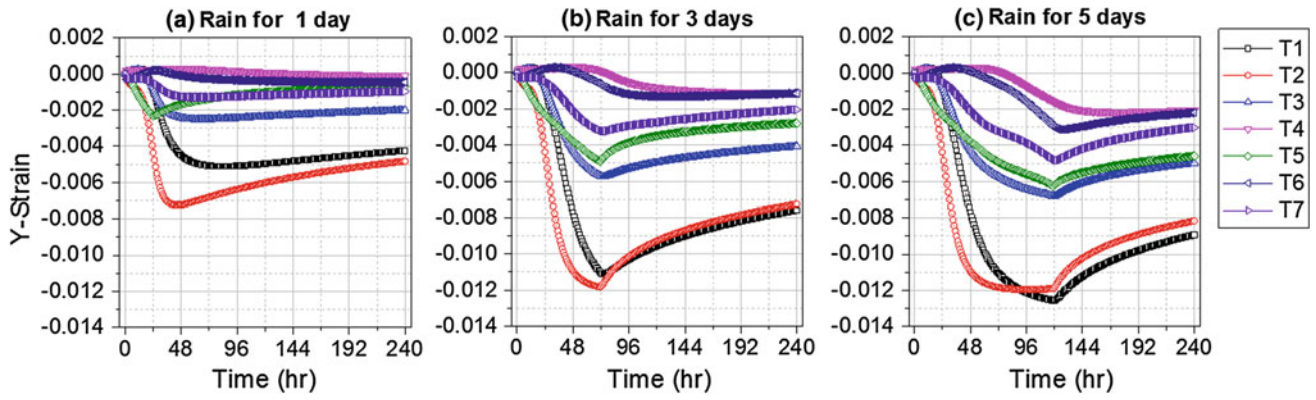


Fig. 7 Magnitude of vertical strains

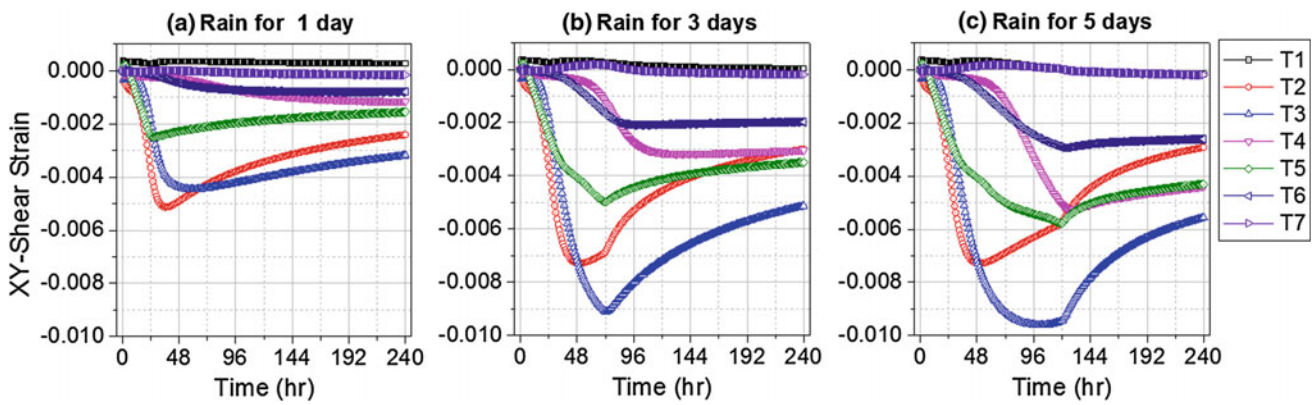


Fig. 8 Magnitude of shear strains

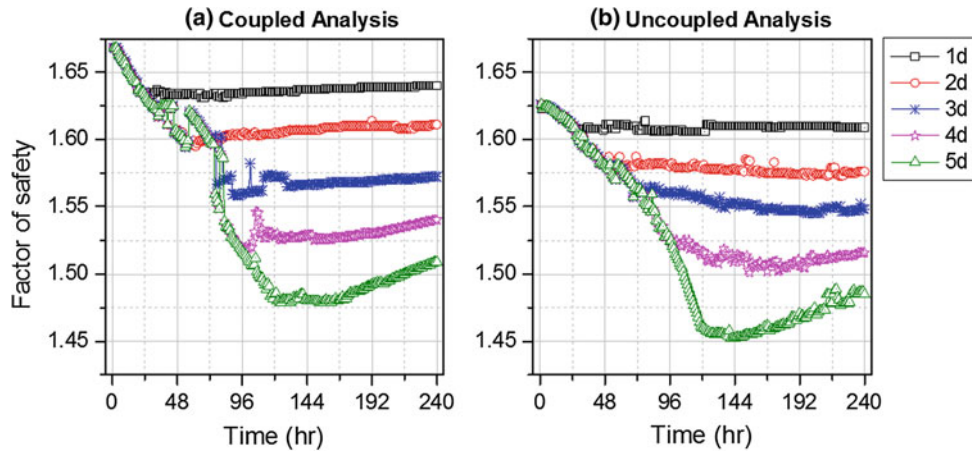


Fig. 9 Variation in factor of safety with rainfall duration

**Table 2** Reduction in factor of safety with rainfall duration for coupled and uncoupled analyses

Duration of rainfall	Coupled analysis (%)	Uncoupled analysis (%)
1 day	3.66	0.98
2 days	1.68	1.80
3 days	4.43	1.20
4 days	7.82	2.30
5 days	4.54	4.33
Cumulative reduction	10.62	13.22

## Conclusions

A red-clay slope was subjected to rainfall intensity of  $6.25 \times 10^{-3}$  m/h for rainstorms with durations of 1, 2, 3, 4, and 5 days. Coupled seepage-deformation and uncoupled seepage only analyses were conducted to determine the pore pressure and deformation response of seven monitoring points within the slope. The results indicate that longer duration rainfall events will cause a greater increase in the pore pressures at each of the seven monitoring points. The increases in the pore pressure will cause variations in the unit weight of the slope material resulting in different amounts of deformations along the slope. Specifically, it was found that the toe of the slope would experience compressive horizontal and vertical strains, while the crest of the slope would experience compressive vertical strains and tensile horizontal strains. Moreover, the shear strains along the slope suggested the slope failure would initiate at the crest of the slope. The increase in the pore pressure from the rainfall events also resulted in a decrease in the factors of safety of the slope. Comparison of the factors of safety obtained from the coupled seepage-deformation analysis and the uncoupled seepage only analysis showed substantial differences. In particular, the amount of reduction in the factor of safety on a daily basis was greater in the coupled analysis in comparison to the uncoupled analysis. However, the cumulative reduction in the factor of safety was greater in the uncoupled analysis.

## References

- Brooks SM, Richards KS (1994) The significance of rainstorm variations to shallow translation hillslope failure. *Earth Surf Proc Land* 19(1):85–94
- Dhakal AS, Sidle RC (2004) Distributed simulations of landslides for different rainfall conditions. *Hydrol Process* 18(4):757–776
- Fletcher L, Hungr O, Evans SG (2002) Contrasting failure behavior of two large landslides in clay and silt. *Can Geotech J* 39:46–62
- Fredlund DG, Rahardjo H (1993) *Soil mechanics for unsaturated soils*. John Wiley & Sons, New York
- Fredlund DF, Xing A (1994) Equations for the soil-water characteristic curve. *Can Geotech J* 39:46–62
- Geo-Slope International, Ltd. (2014a) *Seepage modeling with SEEP/W*. Geo-Slope International
- Geo-Slope International, Ltd. (2014b) *Stability modeling with SLOPE/W*. Geo-Slope International
- Geo-Slope International, Ltd. (2014c) *Stress-deformation modeling with SIGMA/W*. Geo-Slope International
- Haugerud RA (2014) Preliminary interpretation of pre-2014 landslide deposits in the vicinity of Oso, Washington, U.S. Geological Survey Open-File Report 2014-1065
- Heark D, Tiwari B, Ahmad S, Stapleton J (2014) Effect of rainfall in matric suction and seepage in clay slopes. *Proceedings of the 12th international symposium on geo-disaster reduction*, vol 1, pp 65–73
- Henn B, Cao Q, Lettenmaier DP, Magirl CS, Mass C, Bower JB, St. Laurent M, Mao Y, Perica S (2015) Hydroclimatic conditions preceding the March 2014 Oso landslides. *J Hydrol* 16:1243–1249
- Keaton JR, Wartman J, Anderson S, Benoit J, De La Chapelle J, Gilbert RB, Montgomery DR (2014) The 22 March 2014 Oso landslide, Snohomish County, Washington. *Geotechnical Extreme Event Reconnaissance (GEER)*, National Science Foundation
- Liu X, Zou L, Song B (2012) Research on unsaturated hydro-mechanical coupling characteristics of slope considering rainfall infiltration and stability assessment. *Disaster Adv* 5 (4):1615–1622
- Lumb PB (1962) Effects of rain storms on slope stability. In: *Symposium on Hong Kong soils*, pp 73–87
- Phommachanh V, Matsuo, N, Inegawa K, Kawai K, Iizuka A, Tiwari B (2014) Application of soil/water/air coupled F.E. code to predict seepage and deformation on sandy slopes. In: *UNSAT 2014 unsaturated soils—research and application*
- Ng C, Shi Q (1998) Influence of rainfall intensity and duration on slope stability in unsaturated soils. *J Eng Geol* 31(2):105–113
- Song X, Xu W, Shao J, Xu R (2002) Stability analysis of unsaturated soil slope under atomized rain. *J Hohai Univ Nat Sci* 30(S6):16–20
- Tiwari B, Lewis A, Ferrar E (2013) Experimental simulation of rainfall and seismic effects to trigger slope failures. *Geotech Spec Publ* 231 (1):448–451
- Tiwari B, Kawai K, Viradeth P (2014) Numerical modelling of deformation for partially saturated slopes subjected to rainfall. *Landslide Sci Saf Geo Environ* 2:281–286
- Tiwari B, Tran D, Ajmera B, Carrillo Y, Stapleton J, Khan M, Mohiuddin S (2016) Effect of slope steepness, void ratio, and intensity of rainfall on seepage velocity and stability of slopes. In: *Proceedings of the geotechnical and structural engineering congress*
- Tran D (2016) Effect of rainfall and seismic activities on compacted clay slopes having different void ratios and inclinations. Master's thesis. California State University, Fullerton
- Tsai T, Wang J (2011) Examination of influences of rainfall patterns on shallow landslides due to dissipation of matric suction. *Environ Earth Sci* 63(1):65–75
- Wang J, Liang B (2010) Affection of rainfall factor to seepage and stability of loess slope. *J Water Resour Water Eng* 21(1):42–45
- Wartman J, Montgomery DR, Anderson SA, Keaton JR, Benoit J, De La Chapelle J, Gilbert R (2016) The 22 March Oso landslide, Washington. *J Geomorphol* 253(1):275–288
- Zhang L, Zheng Y, Zhao S, Shi W (2003) The feasibility study of strength-reduction method with FEM for calculating safety factors of soil slope stability. *Shuili Xue Bao* 45(1):21–27